NON THERMAL CONTINUUM RADIATION AT THE RADIO PLANETS

D. Jones*

Abstract

Following the encounters of Voyagers 1 and 2 with the magnetospheres of Jupiter and Saturn, it became evident that the same types of natural plasma waves are generated as are observed in the Earth's magnetosphere. One such type of radiation is non thermal continuum, which consists of a broad band of electromagnetic noise trapped within the magnetospheric cavities of the planets. The continuum is produced by multiple reflections, between the cavity walls, of narrow band emissions whose sources lie in the density gradients at the walls of the cavity. The sources themselves are electrostatic upper hybrid waves, and various theories have been proposed for converting them into freely propagating electromagnetic waves. The continuum has been used as a means of determining local plasma density. Efforts have also been made to use the narrow band emissions received on spacecraft to perform remote sensing of the source regions.

1 Introduction

Non thermal continuum radiation from the Earth's magnetosphere was first identified by Brown (1973) at frequencies from about 30 kHz to 100 kHz using radio measurements from the IMP 6 satellite. More detailed observations from IMP 6 by Gurnett and Shaw (1973) and later from GEOS and ISEE, by numerous investigators have extended considerably our knowledge of non thermal continuum and have allowed a number of generation theories to be proposed and developed. The major sources of continuum lie on the morning plasmapause and magnetopause. Density gradients seem to have a major role to play in the generation of the radiation. It was realized that the continuum is not actually produced as a continuum at the source, but rather as narrowband emissions which propagate away into the magnetospheric cavity. The magnetosheath and plasmapause act as reflectors for the lower frequency emissions which become trapped, ultimately propagating tailward (Gurnett, 1975; Jones and Grard, 1976). It is the effects of trapping and multiiple reflections within the cavity, of the emissions at different frequencies from multiple and

*Space Plasma Physics Section, British Antartic Survey, Madingley Road, Cambridge, UK

extended sources, which are mainly responsible for smearing out the narrowband emissions into a continuum. Emissions at higher frequencies, which can penetrate the higher density magnetosheath, propagate freely away through the interplanetary medium.

It is most important that the distinction between the narrowband emissions and continuum be borne in mind; it is more difficult to obtain information on the

source mechanism from the latter because most of the characteristics of the source have been blurred. To bring the nomenclature in line with other planetary structured emissions, such as terrestrial kilometric radiation whose free space wavelength is $\lambda \sim 10^3$ m, it was suggested that the narrowband emissions should be termed Terrestrial myriametric radiation, $\lambda \sim 10^4$ m (Jones, 1980).

Observations by Voyagers 1 and 2 at Jupiter and Saturn show the existence of non thermal continuum within their magnetospheric cavities. Also observed are narrowband emissions similar to those seen in the Earth's magnetosphere. It is, therefore, most important, at least within a planetary context, if not within a wider astrophysical sphere, to understand the mechanisms operating in the regions where the source narrowband emissions are generated. The theories which have been proposed for the generation of Terrestrial myriametric radiation are believed to be applicable to the analogous radiations at Jupiter and Saturn, albeit for different plasma conditions and different source locations within their magnetospheres.

Continuum radiation has been extensively used for determining the local plasma density in the vicinity of spacecraft, since its lower cut–off frequency is at the plasma frequency, $f_p = 9N_e^{1/2}$ kHz where N_e = number of electrons/cm^3. It has also been proposed that information in the narrowband emissions, propagating directly from source to satellite, can be utilised to investigate remotely certain source characteristics.

The next Section reviews the observations of non thermal continuum and Terrestrial myriametric radiation (TMR) in the Earth's magnetosphere, and summarizes the various generation theories which have been proposed. It also deals with the use of non thermal continuum and TMR for plasma and source diagnostics. The subsequent Sections deal with observations of the analogous radiations at Jupiter and Saturn.

2 Terrestrial Non Thermal Continuum and Myriametric Radiations

2.1 Observations

The first high resolution spectrogram of Terrestrial non thermal continuum is shown in Figure 1 (Gurnett and Shaw, 1973). The sharp, lower frequency cut–off, at $\sim$ 5.1 kHz, of the spin–modulated continuum, was identified as being at the local electron plasma frequency, f_p, indicating that the radiation is in the left–hand polarised, ordinary (L–O) electromagnetic mode. The lower cut–off at $\sim$ 6.2 kHz of the non spin–modulated continuum was identified as being that corresponding to the right–hand polarised, extraordinary (R–X) mode, which is believed to be produced predominantly by depolarisation effects

on the L–O mode radiation by multiple reflections within the magnetospheric cavity. The harmonic band structure above the R–X cut–off in Figure 1 was considered to be a characteristic of the source.

Gurnett (1975) provided further details of the continuum radiation spectrum, and showed the distinction between the lower frequency (¡30 kHz) trapped component, and the escaping component at frequencies high enough to propagate freely through the magnetosheath and solar wind. Using a direction–finding technique employing the satellite's spinning dipole antenna, most of the escaping radiation was found to be generated just at or beyond the plasmapause from $\sim$ 4 to $\sim$ 14 hours local time, and at the magnetosheath at $\sim$ 6–10 LT. A close association was found between continuum and intense electrostatic bands near f_p. Observations obtained by the Hawkeye 1 and IMP 8 satellites (Gurnett and Frank, 1976) showed evidence of enhanced continuum radiation intensities closely correlated with the injection of very intense fluxes of energetic, 1 $\sim$ 30 keV, electrons in the outer radiation zone. The continuum was again found to come primarily from the dawn side of the magnetosphere, in agreement with the observed dawn–dusk asymmetry in the 1–30 keV electron distribution. It was suggested that the enhanced continuum could, by some linear or non-linear mechanism, be generated by the electrons via interactions with electrostatic plasma waves which are most intense near and immediately outside the plasmapause.

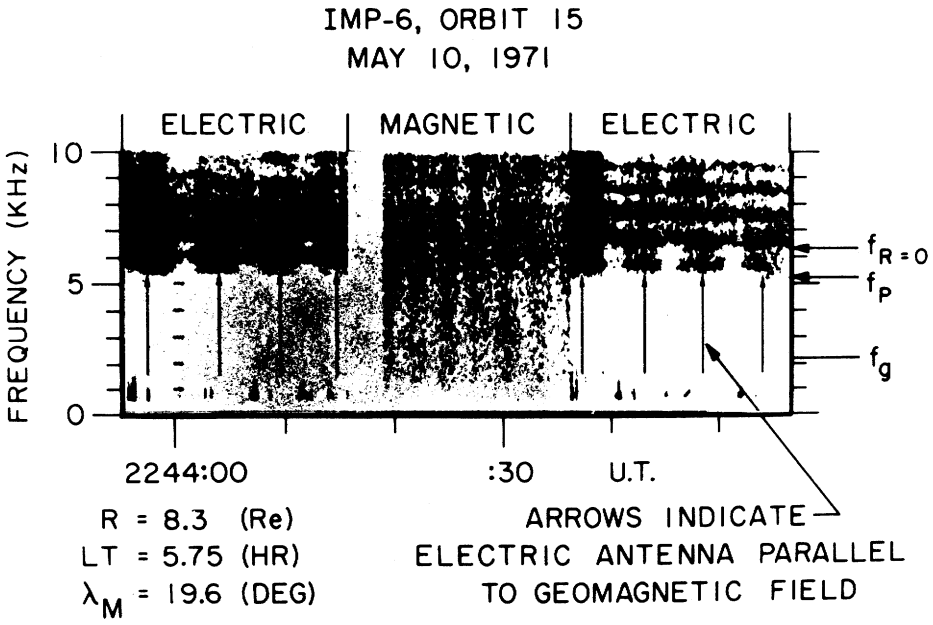

Figure 1: A spectrogram of trapped nonthermal continuum $f > f_p$ showing the occurence of harmonic bands in both electric and magnetic components. The frequency spacing between the bands is not related to the local f_c (from Gurnett and Shaw, 1973).

Significant further advances in understanding non thermal continuum have come from the GEOS and ISEE satellites . Figure 2 shows a spectrogram from GEOS 1, when the satellite was moving inwards towards the plasmapause at $\sim$ 0600 LT. It was proposed that the striated emission band, increasing in intensity as the plasmapause was approached, was Terrestrial myriametric radiation, received directly by the satellite (Jones, 1980, 1981b).

The striations are due to a beat between the spin frequency of the dipole receiving antenna and the sweep frequency of the onboard analyser; the maxima in signal intensity are recorded when the antenna is most closely aligned with the wave electric field.

Kurth et al. (1981a), Jones (1982, 1983a), Gough (1982), and Etcheto et al. (1982) showed further examples of TMR obtained by GEOS and ISEE, in which the emissions are structured in relatively narrow frequency bands, sometimes varying in frequency as illustrated in Figure 3. By this time, evidence had accumulated suggesting that the band spacing should be linked to the electron cyclotron frequency, f_c, at the source. To explain the very narrow band emissions sometimes observed, it was concluded that the source must be compact so that its characteristic frequencies do not vary by a large amount over the emission region.

Kurth et al. (1981a) and Kurth (1982) showed examples relating TMR directly to electrostatic bands near the upper hybrid frequency, $f_{uh} = (f_p^2 + f_c^2)^{1/2}$. Figure 4 shows observations where ISEE encountered large and variable density gradients. Electrostatic upper hybrid waves are observed to be most intense when $f_{uh} \cong (n + 1/2)f_c$ and the steps in frequency of the upper hybrid bands in Figure 4 indicate variations in f_p, since $f_p \gg f_c$. The frequency ripples in the TMR observed by ISEE prior to the upper hybrid emissions may reflect an oscillatory motion of the source . When banded structures are seen in the trapped spectrum of continuum, as in Figure 1, it is assumed that the waves have experienced only a small number of reflections within the magnetospheric cavity and have not diffused in frequency to a large extent; thus they still contain some signatures of their source. Kurth (1982) also observed Z–mode radiation, probably produced as Cerenkov emission, which would undoubtedly provide a secondary, but much weaker, source of TMR (Jones, 1976a, b).

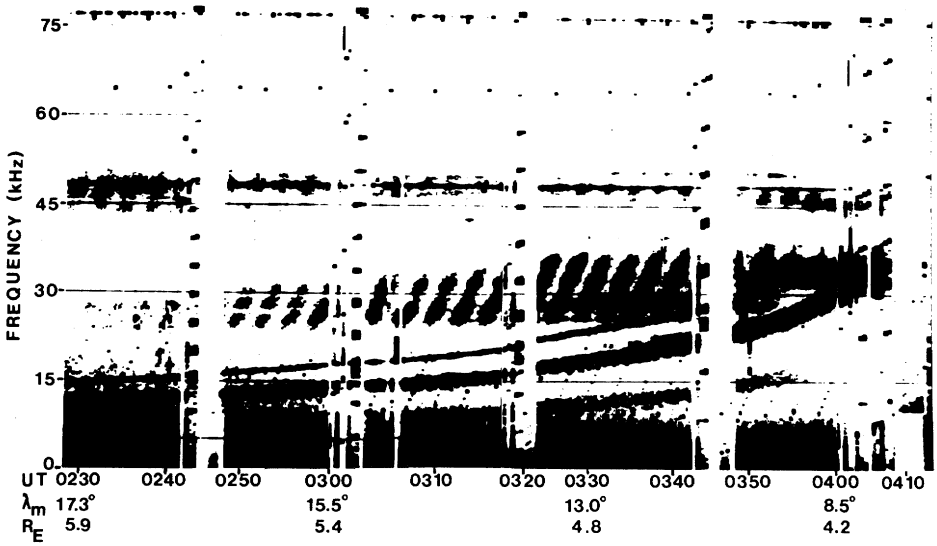

Figure 2: A spectrogram of Terrestrial myriametric radiation obtained on GEOS 1 as it approached the plasmapause; the spin–modulated TMR increases in frequency as time progresses. The intense narrowband emissions increasing in frequency from $\sim$ *15 to* $\sim$ *30 kHz are local electrostatic waves.*

The ratio of the amplitude of the electric field in the upper hybrid bands to that of the

adjacent electromagnetic band is found to be ∼60 in the example shown in Figure 4, as compared to $5{\cdot}10^2$ -10^3 quoted by Okuda et al. (1982) for other events recorded by Kurth et al. (1979c). Kurth (1982) suggests that a difference in density gradients or the effects of beaming could result in the difference in efficiency of conversion from electrostatic to electromagnetic radiation. The lack of direct observational association between some intense upper hybrid waves and TMR had led Kurth et al. (1979c) to propose that strong beaming in particular directions could be occurring. The polarization of the electrostatic bands in Figure 4 was, as expected, with wave electric fields perpendicular to the geomagnetic field. However, the distribution of electric fields was found to be non gyrotropic, indicating that wave vectors at certain angles with respect to the magnetic meridian plane were preferred.

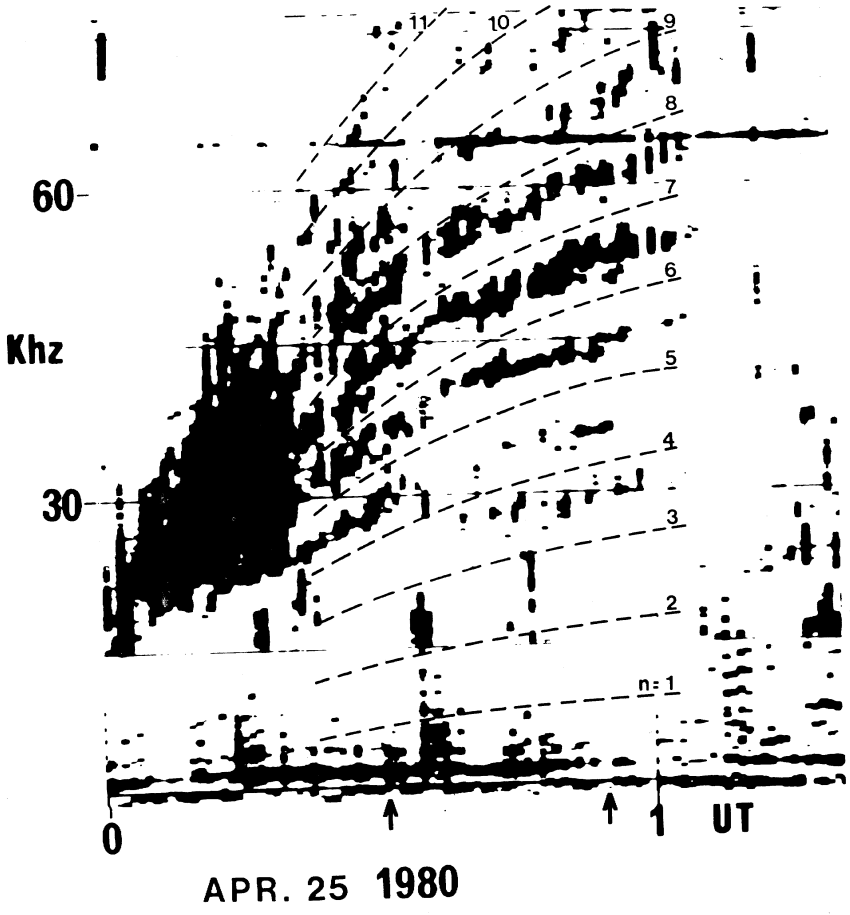

Figure 3: A spectrogram of banded TMR obtained on GEOS 2 at 6.6 R_E, $\lambda_m \sim -3°$. The frequency spacing, which varies with time, can be related to the source f_c.

Besides the plasmapause, other TMR sources have been identified at the magnetopause (Gurnett, 1975). The magnetopause is known to contain electrostatic upper hybrid waves (see, for example, Anderson et al., 1982) and is also a region of density gradients, which appear to be necessary for the mode conversion process. Recent observations of the angular anisotropy of the electric field of continuum by the ISEE–3 satellite at 210 R_e in the geomagnetic tail, show that there appear to be magnetosheath and boundary layer sources of continuum even at these large distances (Coroniti et al., 1984). The detection of

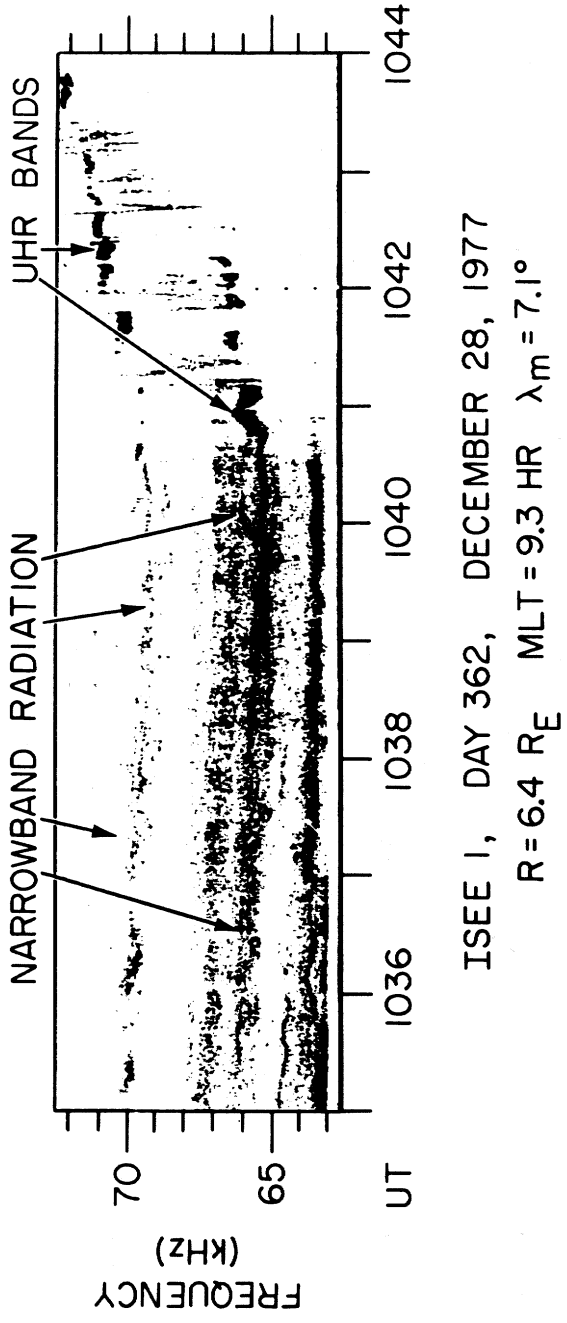

Figure 4: A spectrogram of banded TMR showing a region where electrostatic bands at $(n + 1/2)f_c = f_{uh}$ *are being converted into narrowband TMR near the plasmapause (from Kurth, 1982).*

electron plasma oscillations/upper hybrid emissions by the satellite in the magnetosheath and boundary layer gives support to the suggestion that, as nearer to Earth, the mode conversion of electrostatic waves is important in the production of the electromagnetic waves.

It is clear, therefore, that the major source of TMR lies in electrostatic upper hybrid waves which have been found to be most intense near and immediately beyond the plasmapause. In magnetic latitude, the most intense waves are confined to within a few degrees of the equatorial plane (Gough et al., 1979). Approximately 75% of the emissions used in the GEOS 1 survey were less than 4° in latitudinal extent and 75% were centred between -2° $< \lambda_m <$ 3°. There has been no specific study of electrostatic upper hybrid emissions at the morning–noon magnetopause, although Anderson et al. (1982) have reported the case of an intellse event at $R = 11.2R_E$, $\lambda_m = 0°$, MLT = 11.4 hrs.

Prior to summarizing the various theories which have been proposed for the generation of TMR, some of which involve a beaming of radiation, it is necessary to consider certain other observations which have been made. Etcheto et al. (1982) showed an example of TMR observed simultaneously on GEOS, located at $L = 8.1$, magnetic latitude $\lambda_m = 23°$, magnetic local time MLT = 6.26, and on ISEE, at $L = 8.7$, $\lambda_m = -4.2°$, MLT = 8.03 which, it was claimed, had its source at the plasmapause. On this basis it was concluded that there is not necessarily much latitudinal nor longitudinal beaming or TMR within a solid angle of $\pi/2$ sterad, assuming a source at $\sim 4R_E$, and that this posed serious problems for those theories which advocated beaming.

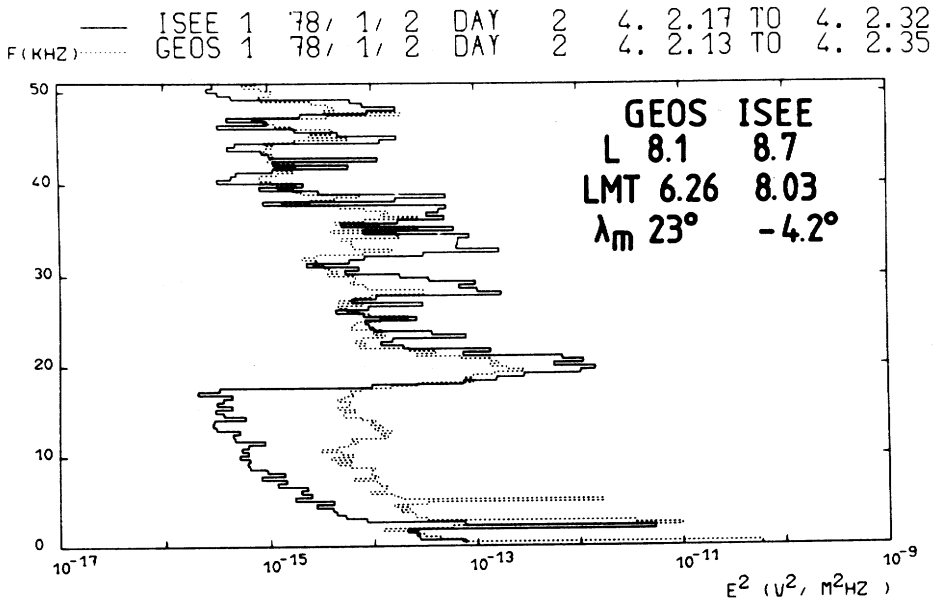

Figure 5: Simultaneous GEOS and ISEE spectra of banded TMR (from Etcheto et al, 1982).

In the event presented by Etcheto et al., the TMR observed by ISEE, the more distant satellite from the plasmapause, was more intense than that recorded on GEOS, as shown in Figure 5, which would appear to indicate a magnetopause rather than a plasmapause source (Jones, 1984b). Considering the ratio of powers recorded and assuming a $1/R^2$

variation in power from source to ISEE and thence to GEOS, results in a source position in the region of $R \cong 12R_E$, $\lambda_m \cong -20°$, MLT $\cong$ 0900. This is very close to the nominal position of the magnetopause and is the region where Gurnett (1975) identified magnetopause sources of TMR as shown in Figure 6. The plasma frequency recorded by ISEE at X in Figure 6 was ∼50 kHz; hence the magnetopause could support TMR in the frequency range shown in Figure 5. Direction–finding measurements with a single spinning dipole as on GEOS and ISEE would clearly be unable to distinguish between such a magnetopause source and one of the plasmapause at $R \cong 5R_E$, MLT = 0500. Further evidence that the source is at the magnetopause comes from the band spacing of the TMR in the spectrogram presented by Etcheto et al., which can be seen to be $<$ 1 kHz. The band spacing is linked to the cyclotron frequency f_c at the source, and the value of $<$ 1 kHz is typical of f_c at the magnetopause, whereas f_c at the plasmapause at $L = 4 - 5$ is $\cong$ 10 kHz. It is also not surprising that the relative bandwidth determined by Etcheto et al. for some of the emission lines should be $\Delta f/f \cong 10^{-3}$, since the Δf needs to be related to $f_c \sim 1$ kHz, i.e. $\Delta f/f \cong 10^{-1}$, which is a typical bandwidth for upper hybrid emission lines (Kurth et al., 1979a).

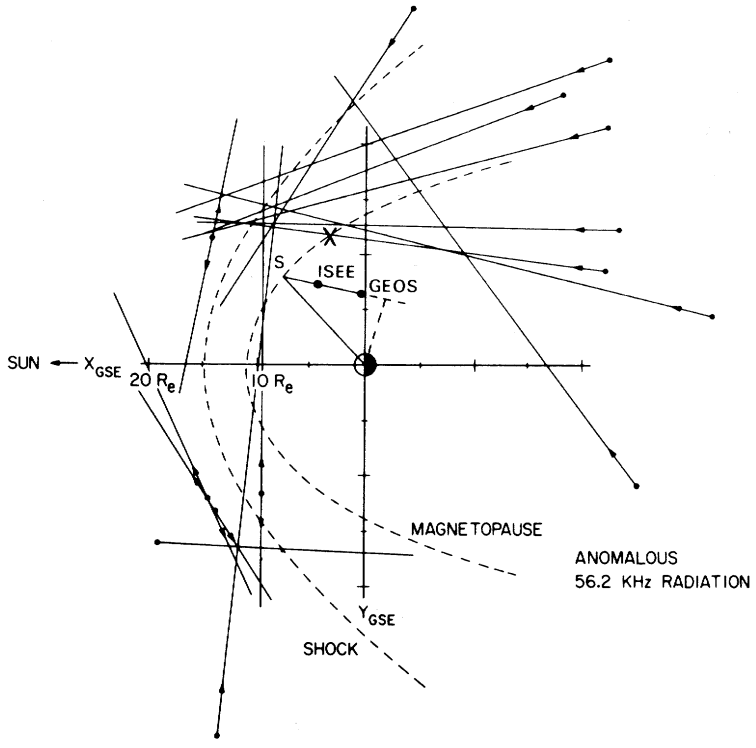

Figure 6: The location of source S of TMR observed simultaneously on GEOS and ISEE (see Figure 5), overlaid on the measurements of Gurnett (1975) of magnetopause sources. The positions of GEOS and ISEE have been projected on to the equatorial plane, whereas the source position is at its computed radial distance. At X, ISEE observed the plasma frequency to be $\sim$ *50 kHz.*

Another puzzle which was presented by Etcheto et al. was of continuum observed on ISEE at frequencies above 200 kHz, trapped within a density trough, and having its lower frequency bound at the R–X mode cut–off. One possible explanation which should be

considered is that the continuum had been produced from terrestrial kilometric radiation (TKR), which appears to be predominantly in the R–X mode (Shawhan and Gurnett, 1982; Mellott et al., 1984). This explanation derives some support from the structured emissions at $\sim$ 200 kHz, which are reminiscent of TMR, seen just prior to the observation of the R–X continuum. In fact, since TKR may extend down in frequency to $<$ 30 kHz (Kurth et al., 1981a) it is not unreasonable to assume that much of the R–X component in trapped continuum, at least down to this frequency, could have derived from TKR.

2.2 Theories for TMR Generation

Following Brown's discovery of NTC, Frankel (1973) proposed synchrotron radiation from trapped, high–energy ($>$ 200 keV) electrons as the source mechanism for continuum. Gurnett and Frank's (1976) observations of the close correlation between continuum and 1-30 keV electron fluxes posed a problem for this theory; it is also found that the power output of the synchrotron mechanism falls short of the required level by a factor of 10^{-2}–10^{-3} (Barbosa, 1982).

A theory proposed by Jones (1976a, b) involved the conversion at a radio window of upper–hybrid Z–mode waves to L–O mode radiation. Upper hybrid noise in the theoretically allowed frequency range $\frac{\left[(f_c^2 + 4f_p^2)^{1/2} - f_c\right]}{2} < f < f_{uh}$ had been observed in the ionosphere and magnetosphere (see, for example, Mosier et al. (1973)), its most likely source being Cerenkov emission. The window theory invoked the propagation of the Z–mode waves in a density gradient such that access was gained to the radio window where the wave frequency equals f_p. Thus the theory had two ingredients later found to be intimately associated with TMR generation: a density gradient and narrow band ($f \sim f_p$) production. When the observational link between TMR and electrostatic waves at $f \sim f_{uh}$ was made (Kurth et al. (1979c)), the theory was further strengthened in that the electrostatic waves lie on the same dispersion branch as the Z–mode (Oya, 1971) and could provide a far more intense source than Cerenkov emission directly in the Z–mode.

Figure 7 shows the dispersion curves of electromagnetic and electrostatic waves for the situation $f_c < f_p < 2f_c$. In the Figure from Lembege and Jones (1982), the frequencies are normalized to f_c; $R_e(k\rho)$ is the real part of the product of k, the wave vector, and ρ, the gyroradius of electrons. The electrostatic part of the dispersion curve is seen to link on to the electromagnetic Z–mode at f_{uh}. Therefore electrostatic waves could, in theory, become Z–mode waves by moving along the dispersion curve to smaller k. This can be achieved by propagation in a density gradient as was shown by Lembege and Jones (1982) for a model plasmapause. The resulting Z–mode radiation, having certain wave normal angles, can then escape via the radio window as originally proposed.

Since the most intense electrostatic upper hybrid waves were observed to be confined to within a few degrees of the magnetic equator at the plasmapause, it was logical to consider that region as being the major source of TMR. It was therefore assumed that the electron density gradient ∇N_e was perpendicular to the geomagnetic field (Jones, 1980), in which case the Z and L–O mode propagation characteristics can be considered by reference to the refractive index surfaces (see, for example, Budden, 1961) in Figure

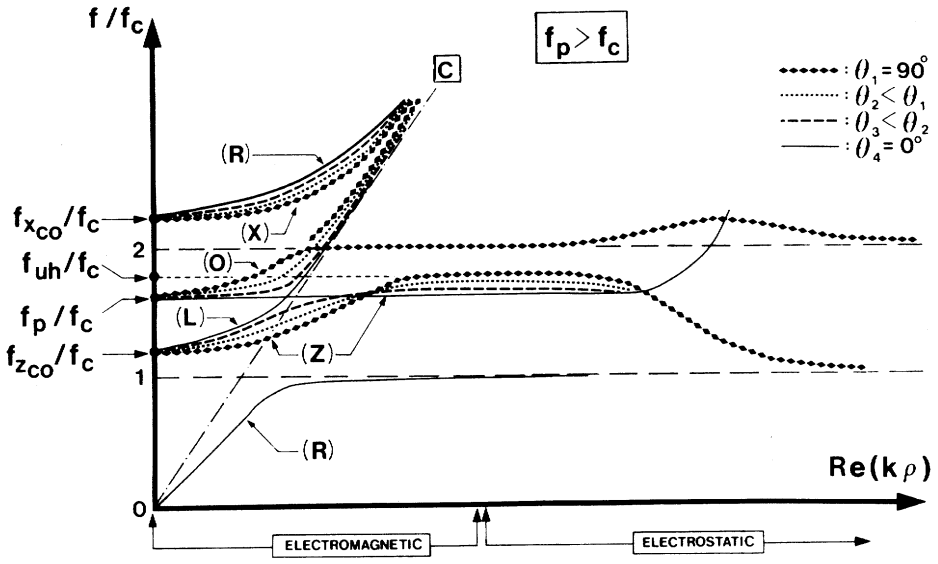

Figure 7: Electromagnetic and electrostatic dispersion curves $Re(\mathbf{k}\rho)$ versus f/f_c for certain wave normal angles from 0° to 90° and for $f/f_c < f_{uh}/f_c < 2f/f_c$.

8. The surfaces are for various plasma densities, with density increasing towards the centre. The points W and W^1 are the windows through which Z–mode waves can escape to become L–O mode radiation; the windows exist at the level where $f = f_p$. Access to the windows is gained by the Z–mode wave having initial wave normal direction n_z in Figure 8, but which started as an electrostatic upper hybrid wave with a much larger wave normal, which would have been nearly perpendicular to B_0 (see Lembege and Jones, 1982). After penetration of the window, the resulting L–O radiation would propagate away to lower densities where $f_p \ll f$, such that the wave normal and resulting ray approach n_0 and r_0 respectively. Hence, assuming a source/window at the magnetic equatorial plasmapause, the L–O radiation will be beamed with respect to the equatorial plane at angle $\alpha = \arctan(f_c/f_p)^{1/2}$ (see Jones, 1980, 1982).

Assuming that the source electrostatic waves are gyrotropic, the efficiency of the conversion via the radio window has been called into question (Barbosa, 1982) because of the small dimensions of the window, which typically correspond to a few degrees in the width of the TMR beam (Jones, 1982). However, if the amplification of the source upper hybrid emissions favoured those waves with wave normals near the $\nabla N_e - B_0$ plane, the efficiency of the process would be greatly increased (Lembege and Jones, i982). The observation by Kurth (1982) of non–gyrotropic upper hybrid waves lends some support to this argument, although it was not possible to determine the relation between the preferred wave normal directions and the $\nabla N_e - B_0$ plane. The direction of ∇N_e is a parameter which is very difficult to determine and it seems that it can have virtually any orientation at the plasmapause, often a highly irregular surface containing field aligned density ducts (see, for example, Carpenter (1978)).

Okuda et al. (1982), and Ashour-Abdalla and Okuda (1984) have considered a linear theory, along the lines proposed by Oya (1974) for the production of Jovian decametric radiation. Oya's theory involves the propagation of electrostatic upper hybrid and Z–

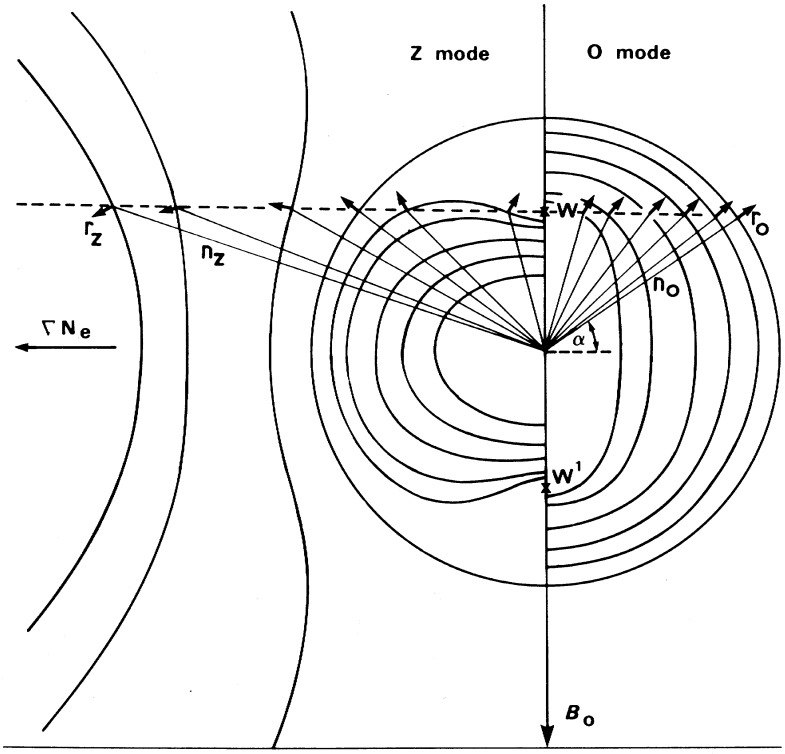

Figure 8: Refractive index curves for the Z and O modes assuming a plasma density gradient ∇N_e perpendicular to the magnetic field B_0 as at the magnetic equator. A Z wave with initial wave normal n_z and corresponding ray r_z passes through the window W to become an O wave finally having wave normal n_O and ray r_O which make angle a with the magnetic equatorial plane.

mode waves in a density gradient, and subsequent mode–coupling through an evanescent region, to L–O mode radiation. It does not invoke a radio window through which the Z–mode radiation is modeconverted into TMR as in the Jones (1976 a,b) theory, and thus would not necessarily result in a beaming of the TMR with respect to the geomagnetic field.

Melrose (1981) proposed that continuum could possibly be produced by the nonlinear coalescence of upper hybrid and low frequency emissions, possibly ion cyclotron waves. Barbosa (1982) indicated that the efficiency of such an interaction would be adequate, but pointed out that there is no observational evidence for the coexistence of the two wave types in what are considered to be TMR source regions. Barbosa suggested that lower hybrid waves should perhaps be considered as the low frequency waves involved in the lnteraction. Ronnmark (1983) further showed that the only low frequency emissions which could possibly be involved in the coalesceIlce process are ion Bernstein waves at high harmonics near or above the lower–hybrid frequency.

Christiansen et al. (1984) state that although the random phase approach used by Ronnmark to calculate the total radiated power is able to account for the power in continuum it cannot describe the fine spectral features observed in TMR. The random phase description is only valid for homogeneous turbulence, while the observations indicate that the

structured radiation originates from highly localised regions containing large amplitude electrostatic waves. They therefore suggested multiple collapsing upper hybrid cavitons interacting with lower frequency waves as a possible source mechanism.

At this stage, therefore, it seems that the linear theories require further studies of their conversion efficiency and further evidence for possible beaming effects (see later). The non–linear theories have yet to be developed in detail and require observational evidence for the coexistence of the ingredients necessary for the wave–wave interactions being proposed.

It is not the purpose of this paper to treat the electrostatic upper hybrid emissions in a detailed theoretical study. The current theories utilise an electron distribution function with two or more components and are based on the Harris dispersion relation (Harris, 1959) for electrostatic waves propagating in a hot plasma with an imbedded magnetic field (Ashour-Abdalla and Kennel, 1978; Hubbard and Birmingham, 1978; Ronnmark et al., 1978). Besides these basic theories, a recent investigation by Engel and Kennel (1984a) of how refractive effects may control the wave amplification has important implications for the theories of TMR production. Engel and Kennel show that the refraction due to the dipole magnetic field, which was neglected in earlier computations (Horne et al., 1981; Ronnmark and Christiansen, 1981), will remove the waves from resonance with free energy source electrons relatively quickly, thereby reducing the amplification process. The refractive effects only become important beyond about 2° of the magnetic equator. To counteract the magnetic field refractioll, Engel and Kennel suggest a plasma density gradient parallel to the geomagnetic field and directed towards the equator. In this way, they achieve the growth rate required to explain the observations of Horne et al (1981) and Ronnmark and Christiansen (1981) which were made at $\lambda_m \cong 10°$. The direction of the k–vector for maximum amplification is found to be perpendicular to the magnetic meridian plane. This would not be conducive to the subsequent propagation of waves through the radio window, unless the density gradient perpendicular to the geomagnetic field were also in that direction. However, in the event studied by Horne et al. and Christiansen et al., no TMR was observed, which may indicate that one requires a different set of conditions for its generation. Also, as stated by Engel and Kennel (1984b), the parallel gradient that favours amplification is opposite to that expected from diffusive equilibrium and is required to have a certain critical value for the waves to achieve the required amplification. This could possibly be achieved sporadically by having a turbulent plasmapause, but it appears difficult to explain such long lasting TMR events as are shown in Figures 2 and 3 on this basis.

2.3 Plasma Diagnostic Using NTC and TMR

Given that non thermal continuum is emitted predominantly as L–O mode myriametric radiation, its lower frequency cut-off s e at $f \cong f_p$ local to the satellite. This assumes that TMR at $f < f_p$ has been produced somewhere along the walls of the magnetospheric cavity; it also assumes that the continuum has suffered sufficient multiple reflections as to have an isotropic wave normal distribution, wlth some wave normals parallel to the local plasma density gradient. In most cases these conditions appear to be satisiied, although

occasionally where, for example, the low frequency cut-off of NTC was approximately constant and independent of satellite location (Gurnett et al, 1976; Coroniti et al, 1984) the cut-off appeared to be determined by non local effects between the source and the satellite.

It is clear that TMR, as distinct from continuum, cannot be used for local plasma diagnostics. However, attempts have been made to utilize it for obtaining information on the source, assuming the linear windos; theory to be valid (Jones, 1980 r 1981b, 1982, 1983a). The technique involves remote sensing of the source region on the assumption that the TMR observed in the magnetospheric cavity has been beamed at angle $\beta = \arctan(f_p/f_c)^{1/2}$ with respect to the geomagnetlc field at the source. For example, assuming a dipole magnetic field model and knowing the position of a satellite which is observing TMR of frequency f, the possible source having $f_p = f$ lies on a certain surface in space. If the wave normal of the TMR at the satellite could be determined accurately, the source position on the surface could be located and the direction of the density gradient at the source obtained, since the radiation is emitted in the $\nabla N_e - B_0$ plane. Unfortunately, no such wave normal determinations yet exist and the use of direction finding based on the spinning dipole technique for such measurements is subject to uncertainties due to polarisation effects (Lecacheux et al, 1979; Jones, 1983a). However, it can be shown that the TMR illustrated in Figure 2, for example, has its most likely source at the plasmapause at $\lambda_m \cong 4°$, this value giving better agreement with the on–board sounder than $\lambda_m \cong 0°$; a plasma density profile of the source region can be obtained along the lines outlined by Jones (1980). In a similar fashion, the banded TMR in Figure 3 is consistent with a source at $R \cong 4.2R_E$, $\lambda_m \cong 3 - 4°$ at 0033 UT, which moved inwards to $R \cong 3.9R_E$, $\lambda_m \cong 3 - 5°$ at 0057 UT, assuming source and satellite lie in the same meridian plane. The reason for the broadband nature of TMR in Figure 2 is that the plasmapause density profile is such that f_{uh} lies between nf_c and $(n+1)f_c$ over a relatively large radial distance, whereas the density profile corresponding to Figure 3 is very steep with f_{uh} crossing many gyroharmonic bands in a short radial distance. In Figure 2, the variation in frequency of the lower cut–off of the TMR as the satellite moved towards the plasmapause is consistent with beaming from the radio window, rather than to its emission according to Okuda et al.'s (1982) mechanism. Other examples of TMR consistent with beaming from sources extending up to $\lambda_m \cong 10°$ are given in Jones (1984a, b).

3 Jovian Non Thermal Continuum, Myriametric, and Kilometric Radiations

3.1 Non Thermal Continuuum and Myriametric Radiations

The Voyager 1 mission provided the first opportunity to examine directly plasma waves in Jupiter's magnetosphere. Figure 9 shows wave observations by Scarf et al. (1979), Gurnett et al. (1981c) in the region of the initial magnetopause crossing, which is marked by the onset of strong continuum radiation trapped within the magnetospheric cavity as

at Earth. The lower frequency limit of the continuum, which decreased from 56 kHz to below 1 kHz, was identified as being the local f_p.

Voyager 2 on entering the magnetospheric cavity also recorded continuum similar in characteristics to that observed by Voyager l (Gurnett et al., 1979). In addition, it recorded intense narrowband emissions near the low frequency cut–off of the continuum radiation. Such emissions were also observed by Voyager 2 when outbound and are shown in Figure 10. The frequency variation of the narrowband emissions consisted of discrete steps having a frequency spacing of $\sim f_c$ strongly suggesting that they are upper hybrid emissions. Evidence that such emissions are involved in producing Jovian myriametric and continuum radiations can be seen in lines and discrete features in the continuum.

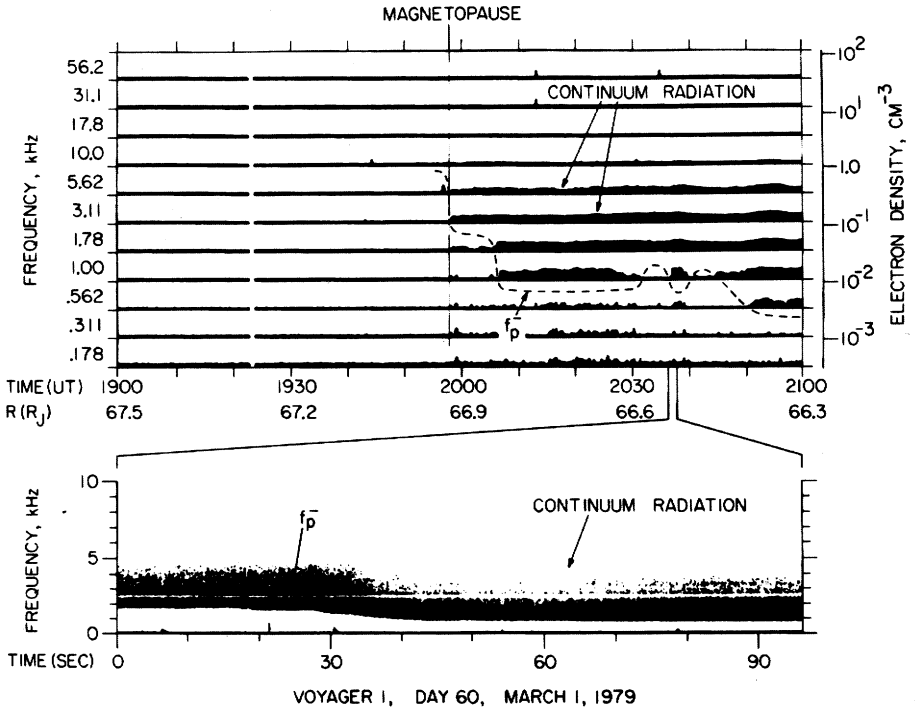

Figure 9: Voyager 1 entry into the Jovian magnetosphere showing the occurrence of trapped continuum. The low–frequency cut–off of the continuum is at the electron plasma frequency f_p, which gives the electron density as shown by the scale to the right of the top panel. The spectrogram in the bottom panel provides high resolution measurements of plasma density (from Gurnett et al, 1981c).

As Voyagers 1 and 2 moved in the magnetospheric cavity towards the inner magnetosphere of Jupiter, the lower frequency cut–off of relatlvely steady continuum was used to determine the plasma density profile (Gurnett et al., 1981c). The average density was found to be higher for V1, $\sim 3 \cdot 10^{-2}$ m^{-3}, than for V2, $\sim 1 \cdot 10^{-2}$ m^{-3}, indicating a more compressed magnetosphere in the former case consistent with the final entry of Voyager 1 into the magnetosphere much closer to the planet, 46.7 R_J as compared to 61.9 R_J for Voyager 2. Voyager 1, on its inbound path in the magnetospheric cavity, observed two events of narrowband emissions at frequencies well above the local f_p (Gurnett et al., 1983). Figure 11 shows a sequence of spectrograms obtained near 42 R_J. Occasionally, as in Figure 11d at 7.4, 8.3 and 9.2 kHz, a series of line emissions can be identified that

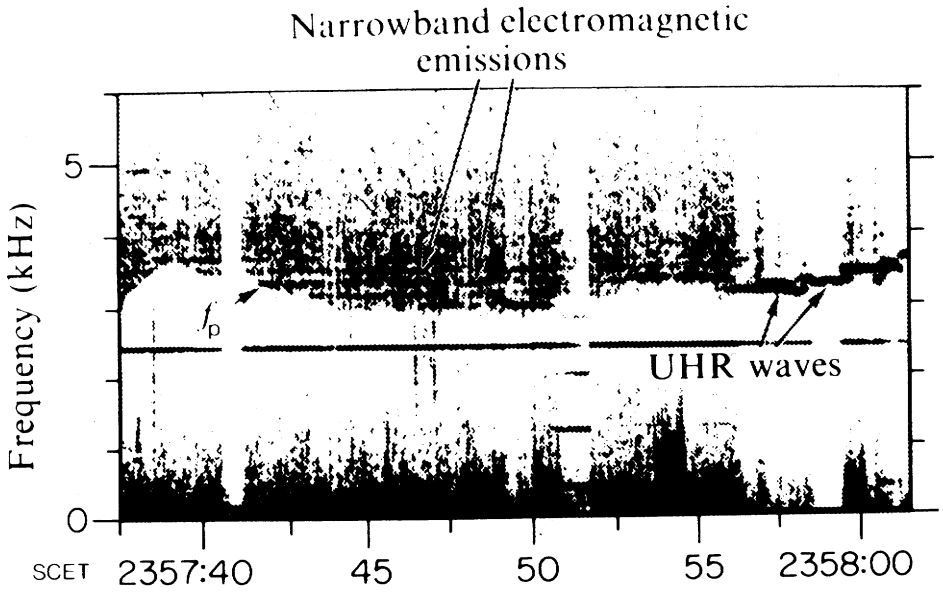

Figure 10: A spectrogram of banded Jovian myriametric radiation (JMR) detected near the magnetopause during the Voyager 2 encounter (4 July, 1979, $R = 71.5R_J$, $\lambda_m = 5.6°$, $LT = 10.3$ h). Also seen are upper hybrid emissions occurring at discrete frequencies separated by the electron cyclotron frequency (from Gurnett et al, 1983).

have a nearly constant frequency spacing, suggesting that the emission frequencies are harmonically related. Based on the average plasma density profile obtained by Gurnett et al. (1981c), the narrowband emissions could have been generated at the magnetic equator near 21 R_J, where $f_c \cong 0.9$ kHz. It is interesting to note that remote sensing on the basis of the window theory yields an average source position for the emissions at $\sim 22R_J$, assuming source and spacecraft lie in the same magnetic meridian plane, the source being assumed to lie in the equatorial plane.

The other narrowband event observed by Voyager 1 when outbound at $\sim 32R_J$ was more complex, the emissions sweeping downward in frequency but having no distinguishable harmonic relationship. Gurnett et al. (1983) suggest that the downward drift is indicative of a cloud of plasma moving outwards, or a transient cloud decaying in density at a fixed radial distance. Remote sensing for this event will require the use of a Jovian magnetic field model which describes conditions beyond the Io plasma torus, taking into account the Jovian current sheet (Connerney et al., 1981).

As Voyagers 1 and 2 reached and traversed the inner magnetosphere other plasma wave emissions were identified, including intense electrostatic waves near half–integral harmonics of f_c, i-e. at $3f_c/2$, $5f_c/2$ and at f_{uh} (Scarf et al., 1979; Gurnett et al., 1979; Scarf et al., 1981a). The upper hybrid emissions were observed primarily at radial distances inside of 25 R_J. In virtually every case the electrostatic emissions were found to occur very close to the magnetic equator, although Warwick et al. (1979a) reported upper hybrid waves in the frequency range 328–385 kHz, in the Io plasma torus when Voyager 1 was at $\sim 5°$ magnetic latitude. Kurth et al. (1980a) noted that there may be local time asymmetries in the amplitudes of cyclotron harmonic emissions in that an intense upper

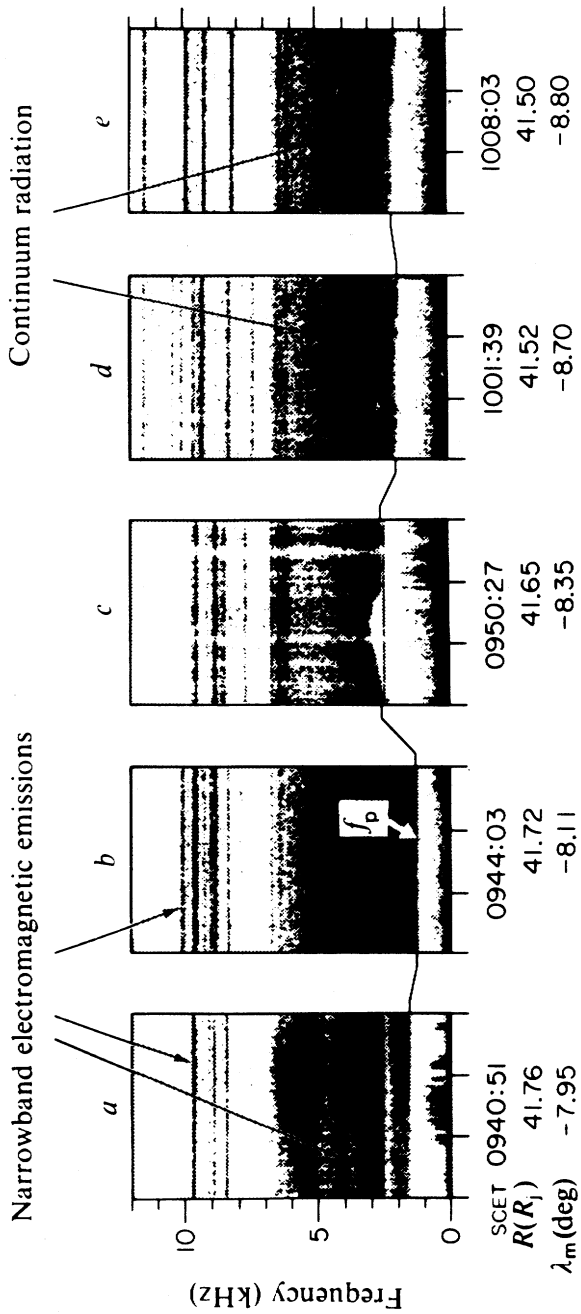

Figure 11: Spectrograms of banded JMR observed by Voyager 1 when inbound. The broadband emission just above f_p is trapped continuum radiation (from Gurnett et al, 1983).

hybrid emission was observed on Voyager 1 when on the dayside but not on the nightside. Within the Io torus, where non thermal continuum was not observed, the upper hybrid emissions provided a userul estimate of f_p and hence of plasma density.

Non thermal continuum cut–off measurements during the outbound passes of Voyagers 1 and 2 provided information on the plasma sheet and boundary layer. Figure 12 shows the entire outbound pass of Voyager 1, in which the most prominent plasma wave phenomenon is the continuum (Gurnett et al., 1980). In fact, the continuum reached intensities in these regions which were among the highest of all wave activities recorded at Jupiter (Barbusa, 1981). Near the planet one may see the well defined $\sim$ 10 hour modulation corresponding to encounters with the high density regions of the plasma sheet, whereas the low density regions correspond to the tail lobes. Beyond 70 R_J there is a transition to a region of nearly constant density which Gurnett et al. interpret as a large increase in the thickness of the plasma sheet. This region they call the boundary layer, being positioned between the inner, rotation–dominated magnetosphere and the magnetopause.

Observations of continuum by Voyagers 1 and 2 at very large distances from Jupiter (Kurth et al., 1981b, 1982b; Scarf et al., 1981b), have led to the identification of brief encounters with the Jovian magnetosphere at distances greater than 700 R_J and in directions substantially away from the Jupiter–Sun line. In addition, a number of examples of continuum, apparently trapped in local density depressions in the solar wind, were observed. Kurth et al. (1981b) suggest that the distant Jovian tail may consist of filamentary structures or that the tail may be offset by the effects of high speed solar wind streams. Scarf et al. (1981b) detected continuum, resembling that of Jupiter, at 6200 R_J $\cong$ 3 AU when Voyager 2 was approaching Saturn. They argue that if there is a leakage of continuum radiation into low density solar wind troughs along the whole tall, it is unlikely that the continuum observed at 3 AU was produced near Jupiter, but rather generated by mode conversion from upper hybrid waves all along the magnetopause.

3.2 Jovian Kilometric Radiation

Some months before encounter, Voyager 1 started to observe wideband radiation in the kilometer wavelength range. Since the frequencies involved ($\sim$ 20 kHz–hundreds of kHz) were similar to those of upper hybrid waves later observed in the Io torus, it was proposed that the torus could be the source region (Warwick et al., 1979a). During its approach to Jupiter, Voyager 2 observed frequencies extending up to and above 1 MHz which would require a higher density torus than was observed by Voyager 1. Although the Io torus was probably more dense during the Voyager 2 encounter it is not clear whether fuh could approach 1 MHz (Warwick et al, 1979b). Both the Io torus and polarauroral field lines have been proposed as sources of broadband Jovian kilometric radiation (Kurth et al., 1979b, 1980; Jones, 1980, 1981a; Green and Gurnett, 1980).

In addition to the broadband kilometric radiation, Voyagers observed kilometric radiation of much narrower bandwidth, typically 40–80 kHz in the 60–150 kHz range (Warwick et al., 1979b). Figure 13 shows a spectrogram obtained when Voyager 1 was $\sim$ 160 R_J from encounter (Kaiser and Desch, 1980). The lower panel represents the total power and the

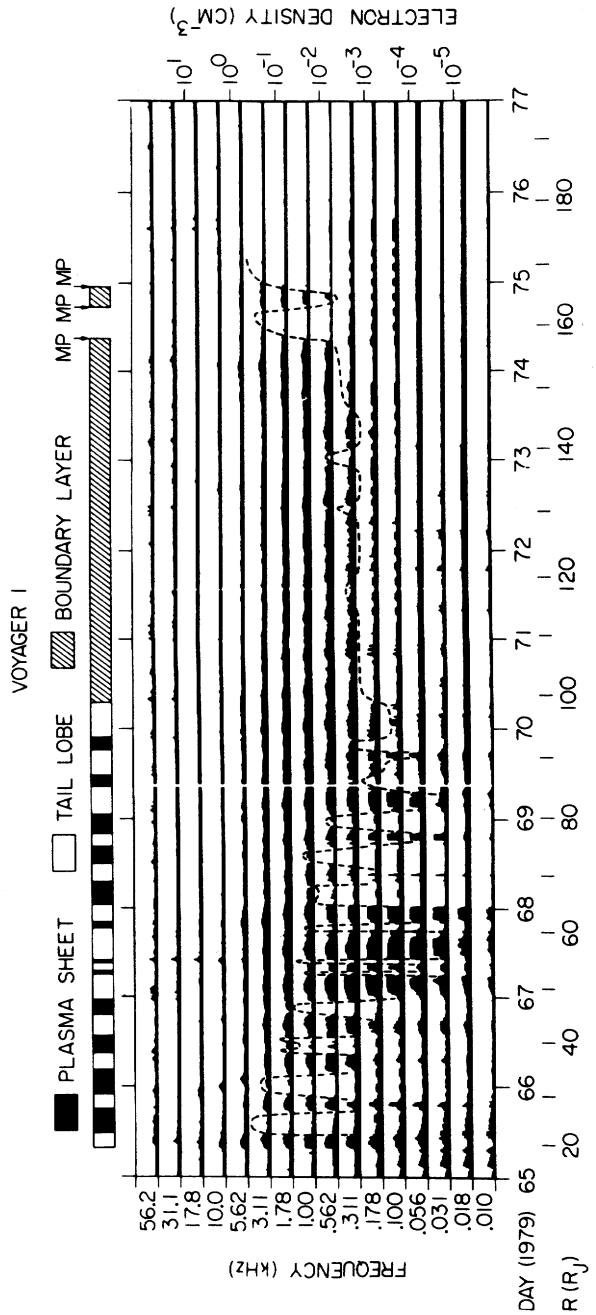

Figure 12: Voyager 1 plasma wave electric field data fron the outbound pass through the magnetotail. The dashed line indicates the electron density profile obtained from the low frequency cut–off of the continuum radiation (from Gurnett et al, 1980).

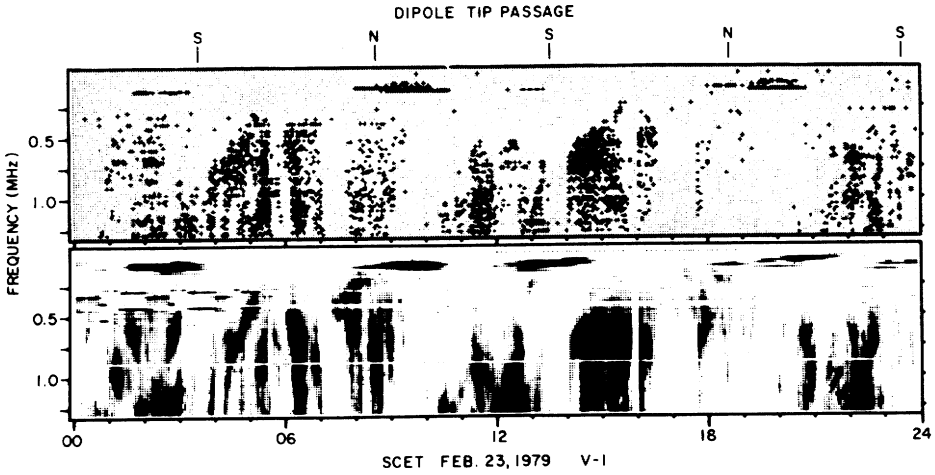

Figure 13: Spectrograms from the Voyager 1 Planetary Radio Astronomy instrument covering the frequency band from ∼0–1.3 MHz. (Note that ordinate scale has frequency increasing downward.) In the lower panel is shown the signal intensity. In the upper panel, left–hand polarized signals appear as black, and right–hand as white. The narrowband JKR events are the intense features near 0.1 MHz (from Kaiser and Desch, 1980).

upper panel the sense of polarization, black being left–hand polarization (radio astronomical definition, i.e. clockwise rotation when the wave is approaching the observer). The narrowband kilometric radiation can be seen near 100 kHz at approximately 02 hr, 09 hr, 14 hr, 20 hr and 23 hr.

The polarization of narrowband kilometric radiation is a function of the observer's magnetic latitude, left–handed in Jupiter's Northern hemisphere and right–handed in the Southern hemisphere. The emission was found not to repeat exactly at the period of rotation of the Jovian magnetic field. During the Voyager 1 encounter, the repetition period was ∼ 1O hr 15 m and during the Voyager 2 encounter it was ∼ 10 hr 28 m. This prompted Kaiser and Desch (1980) to suggest that the source region is at the Io torus where rigid corotation is not expected. The observations would therefore indicate that for long periods of time only one segment of the torus exists. The conditions within the emitting segment must be reasonably constant because of the repeatability of the observed radio spectrum. It is interesting to speculate that, if the source of narrowband kilometric radiation lies in upper hybrid waves, which are observed to be confined near the magnetic equator, and if the conversion process depends on the cold plasma density gradient, which is linked to Jupiter's centrifugal equator (Cummings et al., 1980), the interplay between the two at 8–9 R_J should possibly be taken into account in endeavouring to explain the observations.

4 Saturnian Non Thermal Continuum and Myriametric Radiations

In contrast with the Earth and Jupiter, no detectable non thermal continuum was observed when Voyagers 1 and 2 crossed the magnetopause into Saturn's magnetospheric cavity.

However, a detailed analysis later by Kurth et al. (1982a) of Voyager 1 data revealed the presence of a weak diffuse electromagnetic radiation which was identified as trapped continuum, and which is illustrated in Figure 14; the continuum appears between about 500 Hz and 3 kHz, the lower cut–off being compatible with an f_p corresponding to the local plasma density (Bridge et al., 1981). The average spectrum in the upper panel shows a roll–off at higher frequencies having a spectral index of f^{-3} which can be compared with that in the Earth's magnetosphere of f^{-3} to f^{-6}, and with an average for Jupiter's magnetosphere of $\sim f^{-4}$. It is clear that trapped continuum is not a dominant feature of Saturn's radio spectrum, at least in the regions visited by Voyagers. However, as Kurth et al. point out, both spacecraft were relatively close to the equatorial plane on their inbound trajectories and the plasma sheet densities were equal to or greater than the solar wind density so that no trapped continuum should be recorded in those regions.

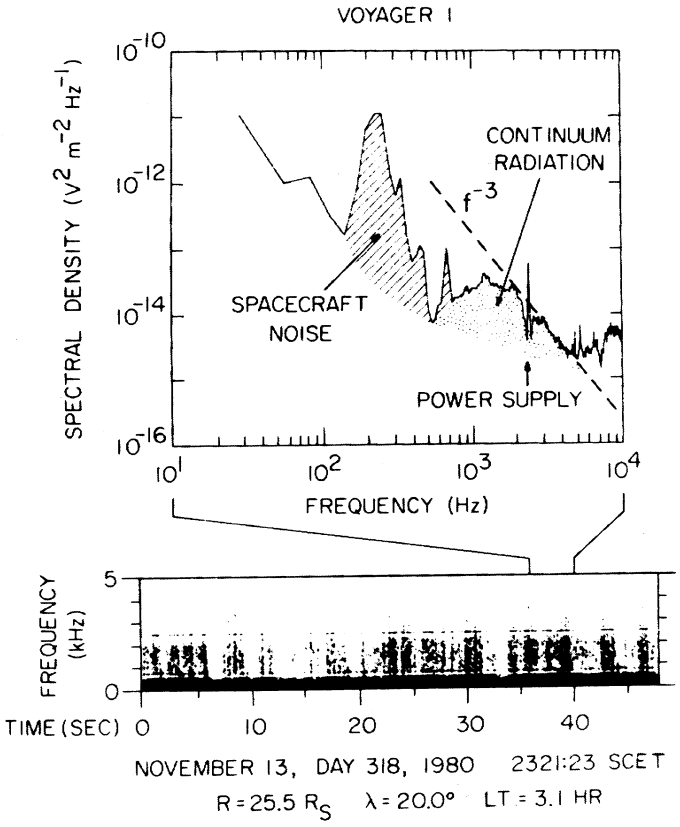

Figure 14: A spectrogram (lower panel) and a 4–sec average spectrum (upper panel) showing the characteristics of continuum radiation trapped within the Saturnian magnetosphere (from Kurth et al, 1982a).

Within Saturn's magnetosphere, the greatest plasma wave activity occurred inside ~ 10 R_S, as illustrated in Figure 15 (Gurnett et al., 1981a). The f_p profile was obtained from an identification of electron plasma oscillations, from upper hybrid emissions, and from the lower cut–off of what are termed as radio emissions in the Figure, which appear to be polarized signals extending upwards in frequency to above 40 kHz (Pedersen et al, 1981). The latter are apparently typical of a distinct narrowbanded component of Saturnian kilometric radiation that is seen intermittently in the Planetary Radio Astronomy receiver on

Voyagers throughout the encounter period. Its characteristics are similar to narrowband Jovian kilometric radiation and it has been suggested that both may originate in the same physical process as for terrestrial myriametric radiation (Warwick et al., 1981).

At lower frequencies the line structure in the radio emission can be seen by reference to the spectrogram in Figure 16A which was obtained near closest approach of Voyager 1 (Gurnett et al., 1981b). The similarity to banded TMR is clear. A similar line seen by Voyager 2 at $\sim$ 6 kHz near closest approach prompted Scarf et al. (1982) to suggest that there exists a source of surprising persistence, bearing in mind that there were nine months between the observations.

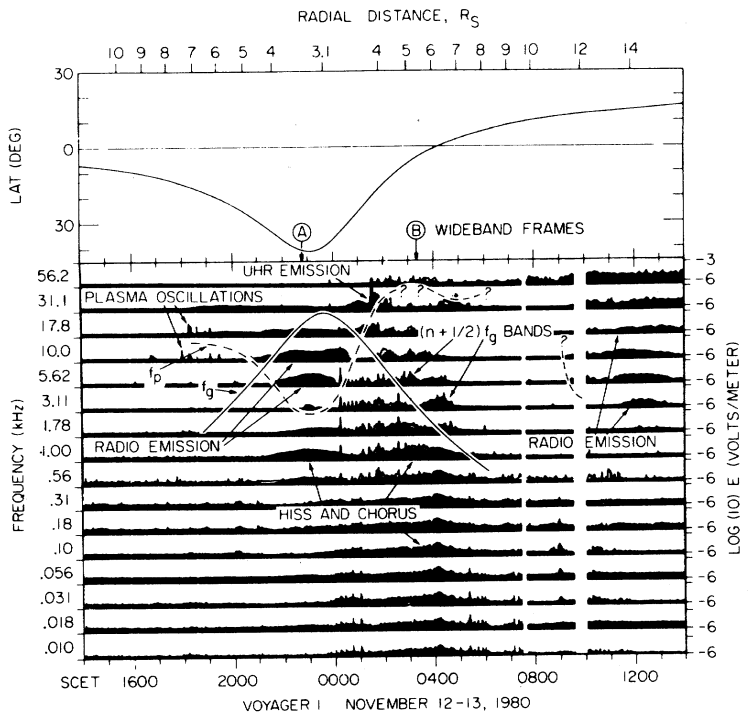

Figure 15: The plasma wave electric field intensities observed by Voyager 1 at Saturn in the region near closest approach. The dashed line gives the approximate plasma frequency f_p profile derived from an identification of electron plasma oscillations, radio emission propagation cut–offs, and upper hybrid emissions (from Gurnett et al, 1981a).

During the outbound leg of the Voyager 1 encounter, persistent bands of emission near 5 kHz were seen from 19 R_S to 58 R_S as shown in Figure 16 B–F. As the plasma parameters varied widely over this range, it is difficult to envisage how the radiation could be anything but freely propagating electromagnetic waves. The meridian plane plot in Figure 17 shows the regions in which the bands were detected. There is evidence for a periodic modulation of the emission intensities, the emissions lasting typically 3–4 hr and tending to recur at Saturn's rotation period of $\sim$ 10 hr. The remote sensing technique developed on the basis of the radio window theory was applied to these emissions (Jones, 1983b) and the most likely source was found to be at $L \cong 10.6$, $\lambda_m \cong 4°$. Although Voyager 1 did not pass through this region, Sittler et al.'s (1983) plasma measurements confirm the existence of a steep plasma density gradient at $L \cong 10.6$ which is interpreted as being due to detachment of plasma outside this boundary.

Electrostatic upper hybrid emissions were observed in Saturn's inner magnetosphere over a whole range of latitudes up to ~ 30, Voyager 1 recorded upper hybrid waves near the magnetic equator at $\sim 5\ R_S$, but there was no marked enhancement as compared to other latitudes. It may be, therefore, that the sources of the radio emissions seen at closest approach by the two spacecraft do not have their origin at the equatorial plane. In fact, the remote sensing technique based on the window theory indicates a Source at $\sim 6R_S$, $\lambda_m \cong 45°$, ($L \cong 13$), where $f_c \cong 4$ kHz, close to the line separation in Figure 16A.

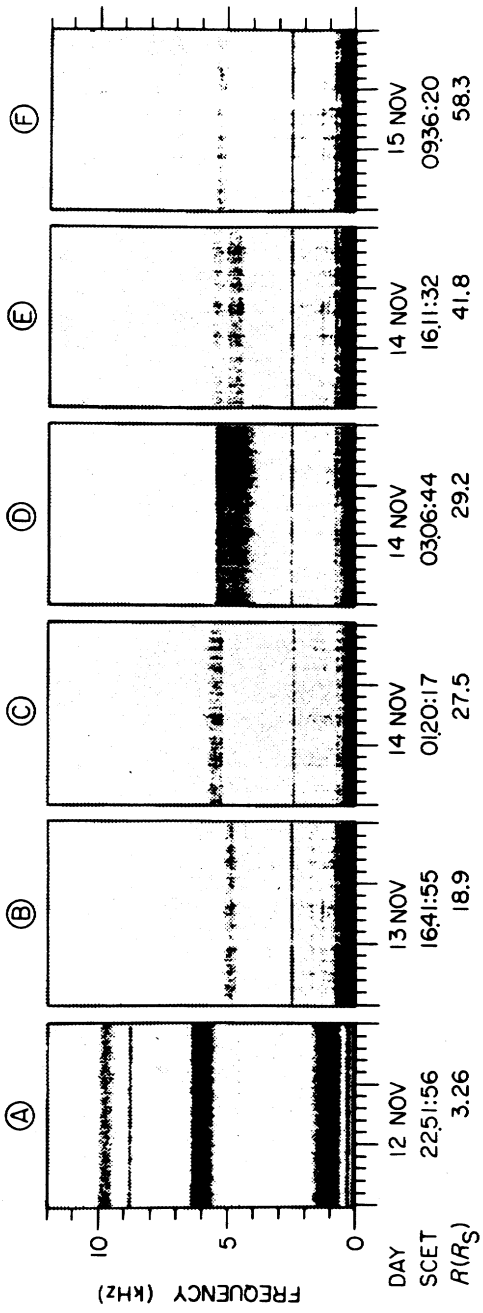

Figure 16: Spectrograms of narrowband Saturnian myriametric radiation (SMR) obtained by Voyager 1 in various regions of Saturn's magnetosphere (from Gurnett et al, 1981b).

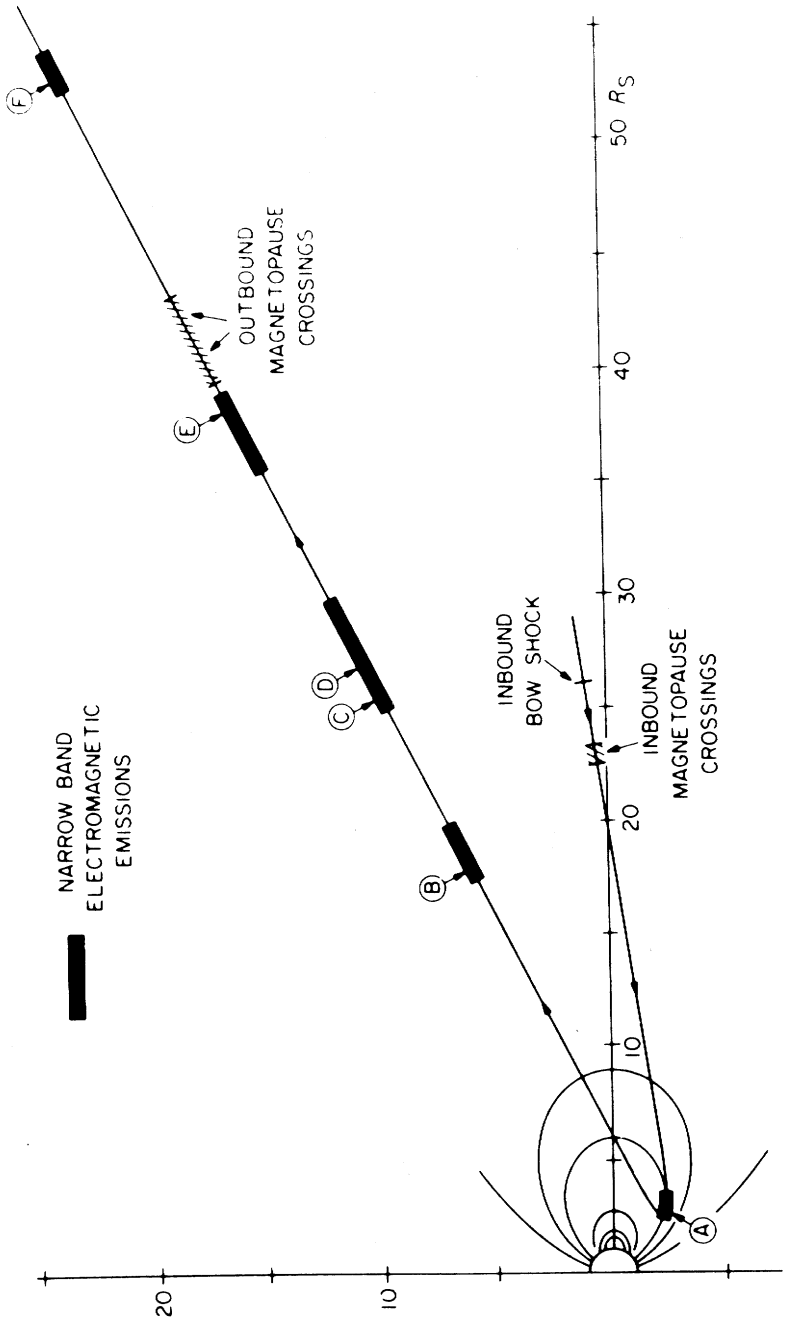

Figure 17: A summary of regions where narrowband SMR were observed. The circles correspond to spectrograms shown in Figure 16 (from Gurnett et al, 1981b).

5 Summary

Non thermal continuum within the magnetospheric cavities of Earth, Jupiter and Saturn is the result of multiple reflections of myriametric radiation, often narrowbanded, from multiple sources located at density gradients at the walls of, and possibly in, the cavity. The myriametric radiation is in the lefthand polarized ordinary mode and the component of non thermal continuum which is right–hand polarized is produced during the multiple reflection process, with possibly a contribution from terrestrial kilometric radiation at higher frequencies. TMR at frequencies too high for trapping will escape through the interplanetary medium.

Tile source of the emissions is electrostatic upper hybrid waves. Plasma density gradients play a crucial role in the conversion process. At Earth, the plasmapause and magnetopause are the important source regions, whereas at Jupiter they are the Io torus and magnetopause; at Saturn the source regions have yet to be determined, but possible candidates are the equatorial plane at $L \cong 10.6$ and in the inner magnetosphere at $\sim 6R_S$, $\lambda_m \cong 45°$. At the Earth and Saturn, the upper hybrid waves are observed over a fairly large magnetic latitude range, although at Earth they are most intense close to the equatorial plane; at Jupiter the e lectrostatic waves are very closely confined to the equatorial plane.

To allow progress to be made regarding the theories which have been proposed requires further investigation and collection of experimental data. The linear conversion theories need an indepth study of the wave distribution functions of the upper hybrid and myriarnetric waves. The non linear theories require observations of the presence, in source regions, of a second wave mode, with which the upper hybrid waves can interact to produce the myriametric radiation. In this case, the existence of non thermal continuum, as distinct from myriametric radiation, near to possible source regions cannot be considered as evidence of generation. Independent of the generation mechanism, the non thermal continuum can be used in most situations to determine local plasma density. However, the use of myriametric radiation for remote sensing of source regions depends on the theory of mode conversion; by adding to the number of cases which have yielded source positions compatible with other observations, the theory and the technique could possibly be validated.

Acknowledgements: The author wishes to thank F. Bagenal, P.J. Christiansen, F.V. Coroniti, F. Genova, C.C. Harvey, C.F. Kennelt, A. Pedersen and E.C. Sittler Jr., for various items of information received.

6 References

Anderson, R. R., C. C. Harvey, M. M. Hoppe, B. T. Tsurutani, T. E. Eastman, and J. Etcheto, Plasma waves near the magnetopause, *J. Geophys. Res.*, **87**, 2087, 1982.

Ashour–Abdalla, M. and C. F. Kennel, Nonconvective and convective electron cyclotron harmonic instabilities, *J. Geophys. Res.*, *83*, 1531, 1978.

Ashour–Abdalla, M. and H. Okuda, Generation of ordinary mode electromagnetic radiation near the upper hybrid frequency in the magnetosphere, *J. Geophys. Res.*, 89, 9125, 1984.

Barbosa, D. D., Fermi–Compton scattering due to magnetopause surface fluctuations in Jupiter's magnetospheric cavity, *Astrophys. J.*, **243**, 1076, 1981.

Barbosa, D. D., Low–level VLF and LF radio emissions observed at Earth and Jupiter, *Rev. Geophys. and Space Phys.*, **20**, 316, 1982.

Bridge, H. S., J. W. Belcher, A. J. Lazarus, S. Olbert, J. D. Sullivan, F. Bagenal, P. R. Gazis, R. E. Hartle, K. W. Ogilvie, J. D. Scudder, E. C. Sittler, A. Eviatar, G. L. Siscoe, C. K. Goertz and V. M. Vasyliunas, Plasma observations near Saturn: Initial results from Voyager 1, *Science*, **212**, 217, 1981.

Brown, L. W., The galactic radio spectrum between 130 and 2600 kHz, *Astrophys. J.*, **180**, 359, 1973.

Budden, K. G., Radio waves in the ionosphere, *Cambridge Univ. Press*, 1961.

Carpenter, D. L., Whistlers and VLF noises propagating just outside the plasmapause, *J. Geophys. Res.*, **83**, 45, 1978.

Christiansen, P. J., J. Etcheto, K. Ronnmark, and L. Stenflo, Upper hybrid turbulence as a source of nonthermal continuum radiation, *Geophys. Res. Lett.*, **11**, 139, 1984.

Connerney, J. E. P., M. H. Acuna, and N. F. Ness, Modelling the Jovian current sheet and inner magnetosphere, *J. Geophys. Res.*, **86**, 8370, 1981.

Coroniti, F. V., F. L. Scarf, C. F. Kennel, and D. A. Gurnett, Continuum radiation and electron plasma oscillations in the distant geomagnetic tail, *Geophys. Res. Lett.*, **11**, 661, 1984.

Cummings, W. D., A. J. Dessler, and T. W. Hill, Latitudinal oscillations of plasma within the Io torus, *J. Geophys. Res.*, **85**, 2108, 1980.

Engel, J. and C. F. Kennel, Effect of parallel refraction on magnetospheric upper hybrid waves, *Geophys. Res. Lett.*, **11**, 865, 1984a.

Engel, J., and C. F. Kennel, The Effects of Density Gradients on the Convective Amplification of Upper Hybrid Waves in the Magnetosphere, *Planet. and Space Sci.*, 1984.

Etcheto, J., P. J. Christiansen, M. P. Gough, and J. G. Trotignon, Terrestrial continuum radiation observations with GEOS-1 and ISEE-1, *Geophys. Res. Lett.*, **9**, 1239, 1982.

Frankel, M. S., LF noise from the Earth's magnetosphere, *Radio Sci.*, **8**, 991, 1973.

Gough, M. P., Non–thermal continuum emissions associated with electron injections: remote plasmapause sounding, *Planet. Space Sci.*, **30**, 657, 1982.

Gough, M. P., P. J. Christiansen, G. Martelli, and E. J. Gershuny, Interaction of electrostatic waves with warm electrons at the geomagnetic equator, *Nature*, **279**, 515, 1979.

Green, J. L. and D. A. Gurnett, Ray tracing of Jovian kilometric radiation, *Geophys. Res. Lett.*, **7**, 65, 1980.

Gurnett, D. A., The earth as a radio source: The nonthermal continuum, *J. Geophys. Res.*, **80**, 2751, 1975.

Gurnett, D. A. and L. A. Frank, Continuum radiation associated with low–energy electrons in the outer radiation zone, *J. Geophys. Res.*, **81**, 3875, 1976.

Gurnett, D. A. and R. R. Shaw, Electromagnetic radiation trapped in the magnetosphere above the plasma frequency, *J. Geophys. Res.*, **78**, 8136, 1973.

Gurnett, D. A., L. A. Frank, and R. P. Lepping, Plasma waves in the distant magnetotail, *J. Geophys. Res.*, **81**, 6059, 1976.

Gurnett, D. A., W. S. Kurth, and F. L. Scarf, Plasma wave observations near Jupiter: Initial results from Voyager 2, *Science*, **206**, 987, 1979.

Gurnett, D. A., W. S. Kurth, and F. L. Scarf, The structure of the Jovian magnetotail from plasma wave observations, *Geophys. Res. Lett.*, **7**, 53, 1980.

Gurnett, D. A., W. S. Kurth, and F. L. Scarf, Plasma waves near Saturn: Initial results from Voyager 1, *Science*, **212**, 235, 1981a.

Gurnett, D. A., W. S. Kurth, and F. L. Scarf, Narrowband electromagnetic emissions from Saturn's magnetosphere, *Nature*, **292**, 733, 1981b.

Gurnett, D. A., F. L. Scarf, W. S. Kurth, R. R. Shaw, and R. L. Poynter, Determination of Jupiter's electron density profile from plasma wave observations, *J. Geophys. Res.*, **86**, 8199, 1981c.

Gurnett, D. A., W. S. Kurth, and F. L. Scarf, Narrowband electromagnetic emissions from Jupiter's magnetosphere, *Nature*, **302**, 385, 1983.

Harris, E. G., Unstable plasma oscillations in a magnetic field, *Phys. Rev. Lett.*, **2**, 34, 1959.

Horne, R. B., P. J. Christiansen, M. P. Gough, K. G. Ronnmark, J. F. E. Johnson, J. Sojka, and G. L. Wrenn, Amplitude variations of electron cyclotron harmonic waves, *Nature*, **294**, 338, 1981.

Hubbard, R. F. and T. J. Birmingham, Electrostatic emissions between electron gyroharmonics in the outer magnetosphere, *J. Geophys. Res.*, **83**, 4837, 1978.

Jones , D ., Mode coupling of Cerenkov radiation as a source of noise above the plasma frequency, The Scientific Satellite Programme During the International Magnetospheric Study, *D. Reidel Publ. Co.*, 281, 1976a.

Jones , D ., Source of terrestrial non-thermal radiation, *Nature*, **260**, 686, 1976b.

Jones , D., Latitudinal beaming of planetary radio emissions, *Nature*, **288**, 225, 1980.

Jones, D., Radio wave emission from the Io torus, *Adv. Space Res.*, **1**, 333, 1981a.

Jones, D., Beaming of Terrestrial myriametric radiation, *Adv. Space Res.*, **1**, 373, 1981b.

Jones, D., Terrestrial myriametric radiation from the Earth's plasmapause, *Planet. Space Sci.*, **30**, 399, 1982.

Jones, D., A technique for studying density gradients and motions of plasmaspheric irregularities, *J. Geophys.*, **52**, 158, 1983a.

Jones, D., Source of Saturnian myriametric radiation, *Nature*, **306**, 453, 1983b.

Jones, D., IMS advances in understanding Terrestrial myriametric radiation, *Proc. Conf. "Achievements of the IMS"*, **ESA SP-217**, 511, 1984a.

Jones, D., Nonthermal continuum – terrestrial myriametric radiation – narrowband electromagnetic emission, in *Results of the ARCAD 3 Project*, CNES, Cepadues Editions, p. 571, Toulouse, France, 1984a.

Jones, D. and R. J. L. Grard, Propagation characteristics of electromagnetic waves in the magnetosphere, in *The Scientific Satellite Programme During the International Magnetospheric Study*, D. Reidel Publ. Co., 293, 1976.

Kaiser, M. L. and M. D. Desch, Narrow–band Jovian kilometric radiation: A new radio component, *Geophys. Res. Lett.*, **7**, 389, 1980.

Kurth, W. S., Detailed observations of the source of Terrestrial narrowband electromagnetic radiation, *Geophys. Res. Lett.*, **9**, 1341, 1982.

Kurth, W. S., M. Ashour–Abdalla, L. A. Frankt, C. F. Kennel, D. A. Gurnett, D. D. Sentman, and B. G. Burek, A comparison of intense electrostatic waves near f_{UHR} with linear instability theory, *Geophys. Res. Lett.*, **6**, 487, 1979a.

Kurth, W. S., D. D. Barbosa, F. L. Scarf, D. A. Gurnett, and R. L. Poynter, Low frequency radio emissions from Jupiter: Jovian kilometric radiation, *Geophys. Res. Lett.*, **6**, 747, 1979b.

Kurth, W. S., J. D. Craven, L. A. Frank, and D. A. Gurnett, Intense electrostatic waves near the upper hybrid resonance frequency, *J. Geophys. Res.*, **84**, 4145, 1979c.

Kurth, W. S., D. D. Barbosa, D. A. Gurnett, and F. L. Scarf, Electrostatic waves in the Jovian magnetosphere, *Geophys. Res. Lett.*, **7**, 57, 1980a.

Kurth, W. S., D. A. Gurnett, and F. L. Scarf, Spatial and temporal studies of Jovian kilometric radiation, *Geophys. Res. Lett.*, **7**, 61, 1980b.

Kurth, W. S., D. A. Gurnett, and R. R. Anderson, Escaping nonthermal continuum radiation, *J. Geophys. Res.*, **86**, 5519, 1981a.

Kurth, W. S., D. A. Gurnett, F. L. Scarf, R. L. Poynter, and J. D. Sullivan, Voyager observations of Jupiter's distant magnetotail, *J. Geophys. Res.*, **86**, 8402, 1981b.

Kurth, W. S., F. L. Scarf, J. D. Sullivan, and D. A. Gurnett, Detection of nonthermal continuum radiation in Saturn's magnetosphere, *Geophys. Res. Lett.*, **9**, 889, 1982a.

Kurth, W. S., J. D. Sullivan, D. A. Gurnett, F. L. Scarf, H. S. Bridge, and E.C. Sittler, Observations of Jupiter's distant magnetotail and wake, *J. Geophys. Res.*, **87**, 10373, 1982b.

Lecacheux, A., C. C. Harvey, and A. Boischot, Source localisation and polarization determination in low frequency satellite radio astronomy, *Annales Telecomm.*, **35**, 253, 1979.

Lembege, B. and D. Jones, Propagation of electrostatic upperhybrid emission and Z–mode waves at the geomagnetic equatorial plasmapause, *J. Geophys. Res.*, **87**, 6187, 1982.

Mellott, M. M., W. Calvert, R. L. Huff, and D. A. Gurnett, DE-1 observations of ordinary mode and extraordinary mode auroral kilometric radiation, *Geophys. Res. Lett.*, **11**, 1188, 1984.

Melrose, D. B., A theory for the nonthermal radio continua in the terrestrial and Jovian magnetospheres, *J. Geophys. Res.*, **86**, 30, 1981.

Mosier, S. R., M. L. Kaiser, and L. W. Brown, Observations of noise bands associated with the upper hybrid resonance by the IMP 6 radio astronomy experiment, *J. Geophys. Res.*, **78**, 1673, 1973.

Okuda, H., M. Ashour–Abdalla, M. S. Chance, and W. S. Kurth, Generation of nonthermal continuum radiation in the magnetosphere, *J. Geophys. Res.*, **87**, 10457, 1982.

Oya, H., Conversion of electrostatic waves into electromagnetic waves: Numerical calculation of the dispersion relation for all wavelengths, *Radio Sci.*, **6**, 1131, 1971.

Oya, H., Origin of Jovian decameter wave emissions - Conversion from the electron cyclotron plasma wave to the ordinary mode electromagnetic wave, *Planet. Space Sci.*, **22**, 687, 1974.

Pedersen, B. M., M. G. Aubier, and J. K. Alexander, Low–frequency plasma waves near Saturn, *Nature*, **292**, 714, 1981.

Ronnmark, K., Emission of myriametric radiation by coalescence of upper hybrid waves with low frequency waves, *Annal. Geophys.*, **1**, 187, 1983.

Ronnmark, K. and P. J. Christiansen, Dayside electron cyclotron harmonic emissions, *Nature*, **294**, 335, 1981.

Ronnmark, K., H. Borg, P. J. Christiansen, M. P. Gough, and D. Jones, Banded electron cyclotron harmonic instability – a first comparison of theory and experiment, *Space Sci. Rev.*, **22**, 401, 1978.

Scarf, F. L., D. A. Gurnett, and W. S. Kurth, Jupiter plasma wave observations: An initial Voyager 1 overview, *Science*, **204**, 991, 1979.

Scarf, F. L., D. A. Gurnett, and W. S. Kurth, Measurements of plasma wave spectra in Jupiter's magnetosphere, *J. Geophys. Res.*, **86**, 8181, 1981a.

Scarf, F. L., W. S. Kurth, D. A. Gurnett, H. S. Bridge, and J. D. Sullivan, Jupiter tail phenomena upstream from Saturn, *Nature*, **292**, 585, 1981b.

Scarf, F. L., D. A. Gurnett, W. S. Kurth, and R. L. Poynter, Voyager 2 plasma wave observations at Saturn, *Science*, **215**, 587, 1982.

Shawhan, S. D. and D. A. Gurnett, Polarization measurements of auroral kilometric radiation by Dynamics Explorer-1, *Geophys. Res. Lett.*, **9**, 913, 1982.

Sittler, E. C., K. W. Ogilvie, and J. D. Scudder, Survey of low–energy plasma electrons in Saturn's magnetosphere: Voyagers 1 and 2, *J. Geophys. Res.*, **88**, 8847, 1983.

Warwick, J. W., J. B. Pearce, A. C. Riddle, J. K. Alexander , M. D. Desch, M. L. Kaiser, J. R. Thieman, T. D. Carr, S. Gulkis, A. Boischot, C. C. Harvey, and B. M. Pedersen, Voyager 1 planetary radio astronomy observations near Jupiter, *Science*, **204**, 995, 1979a.

Warwick, J. W., J. B. Pearce, A. C. Riddle, J. K. Alexander, M. D. Desch, M. L. Kaiser, J. R. Thieman, T. D. Carr, S. Gulkis, A. Boischot, Y. Leblanc, B. M. Pedersen, and D. H. Staelin, Planetary radio astronomy observations from Voyager 2 near Jupiter, *Science*, **206**, 991, 1979b.

Warwick, J. W., J. B. Pearce, D. R. Evans, T. D. Carr, J. J. Schauble, J. K. Alexander, M. L. Kaiser, M. D. Desch, M. Pedersen, A. Lecacheux, G. Daigne, A. Boischot, and C. H. Barrow, Planetary Radio Astronomy observations from Voyager 1 near Saturn, *Science*, **212**, 239, 1981.